

**RESEARCH INTO FLOWS
IN TURBINE BLADE SEALS
PART II: NUMERICAL ANALYSIS**
ROBERT STEPIEŃ¹, KRZYSZTOF KOSOWSKI¹
AND JANUSZ BADUR²

¹*Faculty of Ocean Engineering and Ship Technology,
Gdansk University of Technology,
Narutowicza 11/12, 80-952 Gdansk, Poland
{rstepien,kosowski}@pg.gda.pl*

²*Institute of Fluid-Flow Machinery, Polish Academy of Sciences,
Fiszera 14, 80-952 Gdansk, Poland
jb@imp.gda.pl*

(Received 31 January 2003; revised manuscript received 10 April 2003)

Abstract: 3D calculations of an axial model turbine of the impulse type were performed using the FLUENT CFD code. The calculations were carried out for variants which had been measured experimentally. Special attention was paid to the pressure field in the rotor blade shroud clearance. The Multiple Reference Frame method, the Mixing Plane method and the Sliding Mesh method were applied, and meshes of different types and configurations were used for calculations. Only the Sliding Mesh technique appeared to describe non-stationary effects and pressure pulsations in the turbine flow channels and clearances. In this part of the paper, numerical analysis is described, while the comparison between the experimental and the calculated results is presented in part III.

Keywords: turbine seals, CFD calculations, experimental investigations

1. Modelling of the turbine stage geometry

A cross-section of the turbine, its dimensions, as well as the nozzle and rotor profiles are presented in Figure 1. The geometry of the flow part of the turbine stage was modeled by a calculating mesh. It was divided into four blocks: an inlet to the stage with nozzle channels, rotor blade channels, a shroud clearance and a stage exit. An example of the blocks and the mesh of the flow parts is presented in Figures 2 and 3, respectively. In all the calculated variants the rotor passages were modeled by the moving mesh, and the rotor blades were treated as a “moving wall”. All the other meshes were assumed to be stationary. Meshes of different types and configurations were used for calculations. The differences between the meshes are shown in Figure 4. According to this figure, the particular types of meshes are marked by numbers 1, 2, 3 and 4 respectively. Only the mesh of type 4 is constructed in a nonstructural way for

modelling the geometry of the shroud clearance. Meshes 1, 2, 3 are entirely structural ones. The structural meshes were built with hexahedra cells, while the meshes made in an unstructured way consisted mainly of pyramid cells. Three variants of the mesh blocks and the interfaces connecting them were considered. They are marked A, B, C and presented in Figure 5. Examples of mesh structures used in the calculations are collected in Table 1. They refer to configurations characterized by mesh type (1, 2, 3, 4) and the type of mesh block interfaces (A, B, C). The appropriate numbers of the mesh cells are also shown in Table 1.

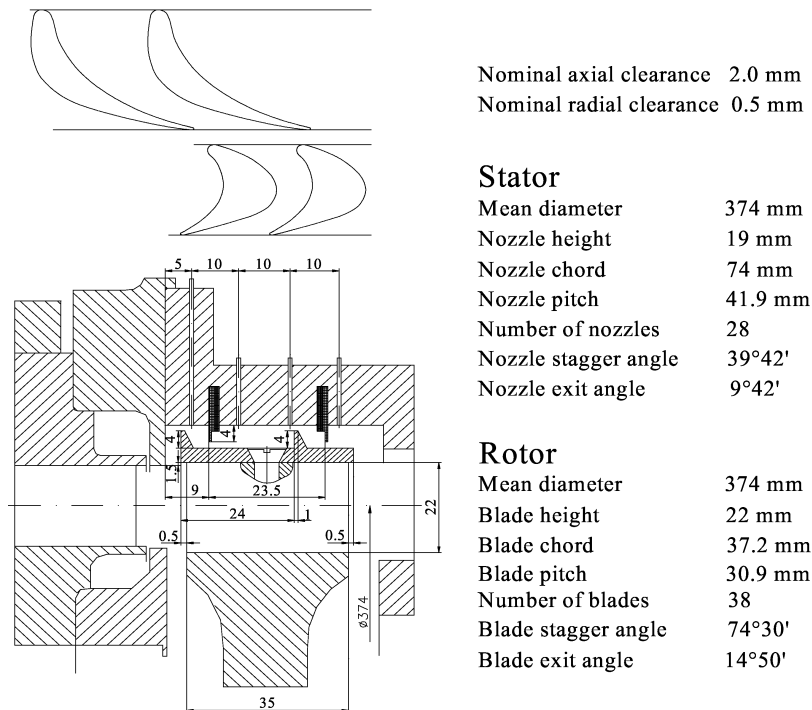


Figure 1. Turbine flow part and the nozzle and rotor profiles

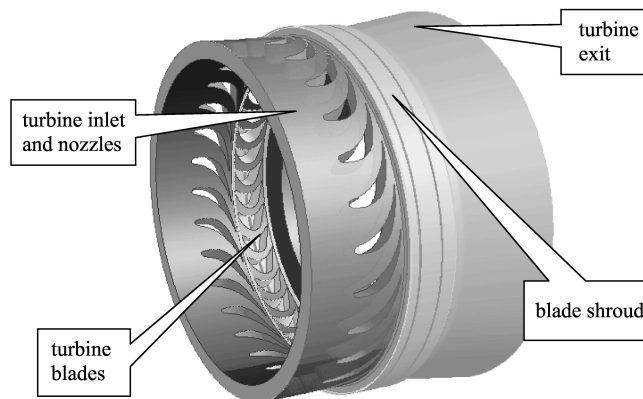


Figure 2. Blocks of meshes representing the turbine flow part (example)

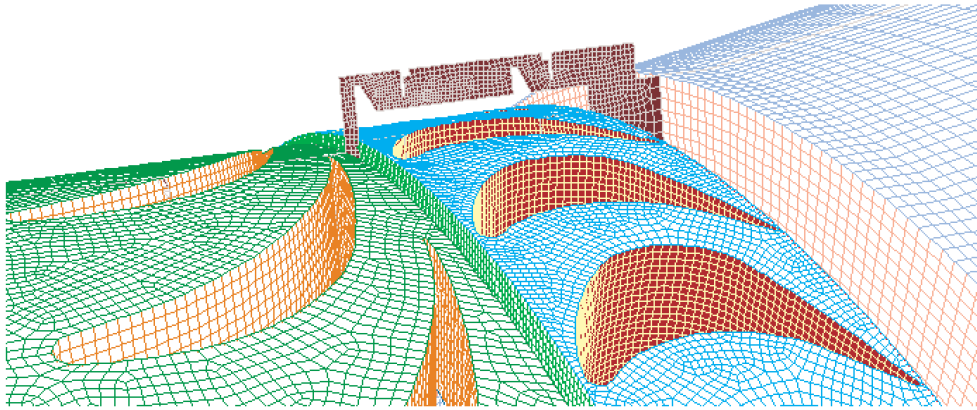


Figure 3. Fragment of stage flow mesh

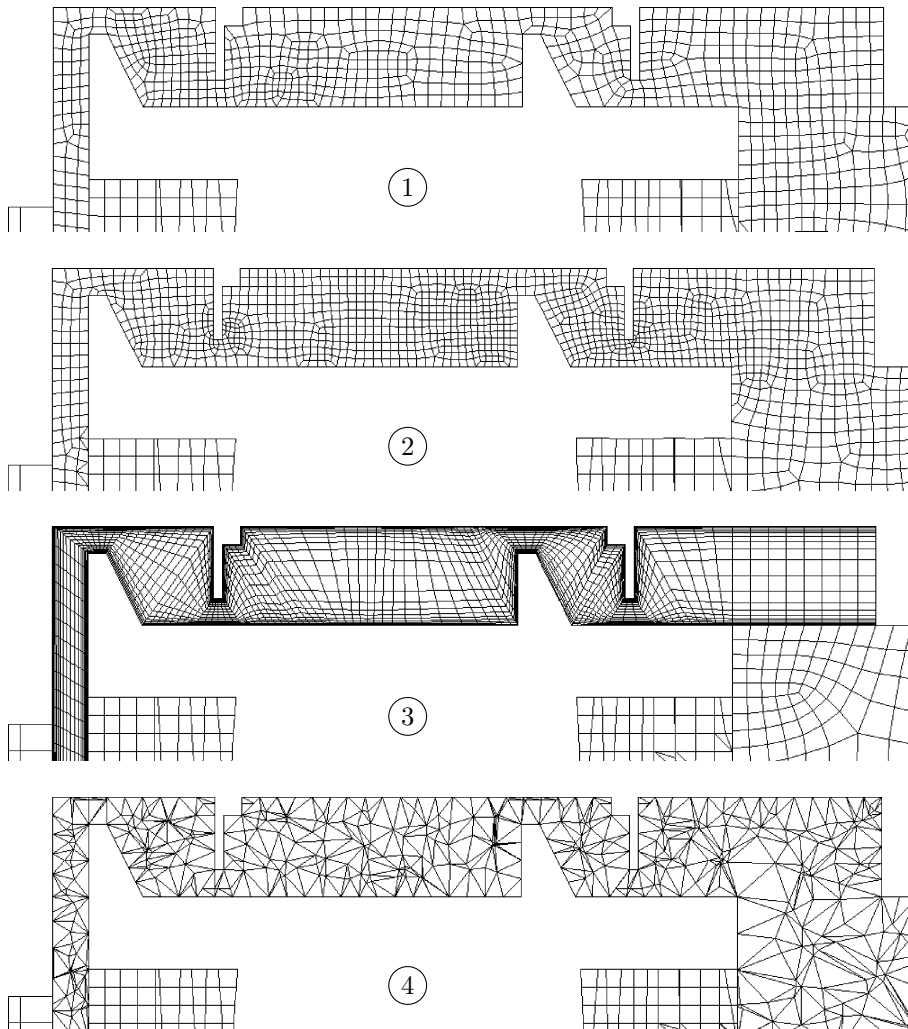


Figure 4. Different types of meshes

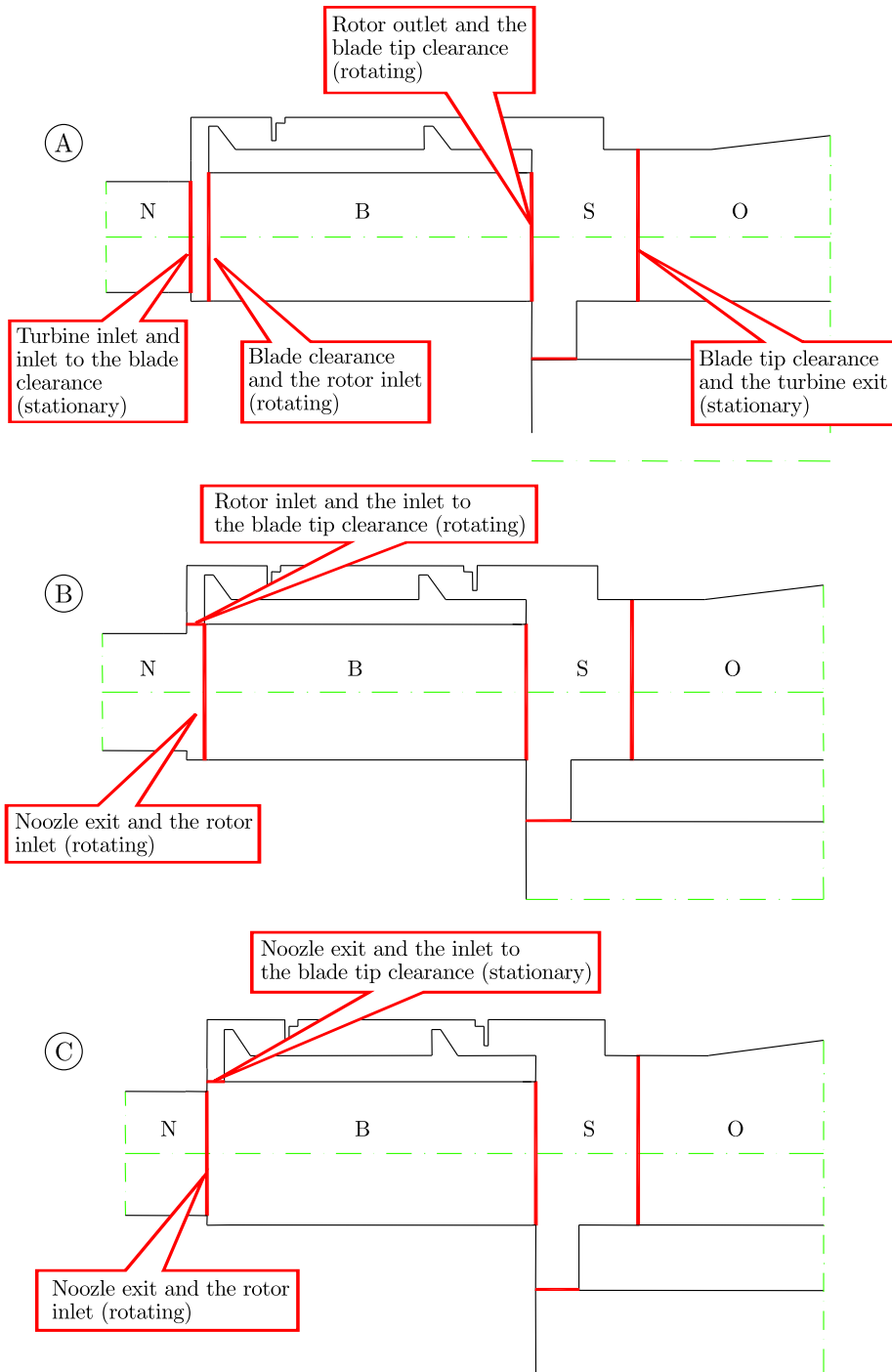


Figure 5. The three variants of mesh blocks and their interfaces (N – stator nozzle, B – rotor blade, S – seal and stage exit, O – turbine outlet)

Table 1. Different variants of mesh type/grid interfaces and the numbers of mesh cells (in thousands); (S) – structural mesh, (NS) – nonstructural mesh

No	Mesh type	Grid interfaces	Seal	Rotor	Stator	Outlet	Total
1	1	A	1050(S)	450(S)	360(S)	185(S)	2045
2	2	A	1640(S)	450(S)	360(S)	185(S)	2635
3	1	C	995(S)	560(S)	360(S)	185(S)	2100
4	1	B	995(S)	450(S)	425(S)	185(S)	2055
5	3	B	1365(S)	450(S)	425(S)	185(S)	2425
6	3	A	1500(S)	450(S)	360(S)	185(S)	2495
7	4	A	1200(NS)	450(S)	360(S)	185(S)	2195

The calculations were carried out for the variants which had been measured experimentally (see part I of this paper). The investigations were performed for various values of rotor speed: $\omega = 311\text{rad/s}$, $\omega = 566\text{rad/s}$ and $\omega = 645\text{rad/s}$. The pressure at the stage inlet was equal to 9, 20 and 24kPa, respectively, above the atmospheric level. These values of rotor speed and inlet pressure were also assumed for the calculations. The calculation methods provided by the FLUENT CFD code, *i.e.* the Multiple Reference Frame method, the Mixing Plane method and the Sliding Mesh method (with a time step equal to $5 \cdot 10^{-5}\text{s}$) were applied for calculations of each variant of the rotor speed and each variant of the mesh geometry. The calculations were performed assuming non-flow initial conditions and a gradual rotor speed increase, starting from a standstill. For the Sliding Mesh method calculations were repeated using the results obtained by the Multi Reference Frame technique as initial conditions. In this case, the assumed accuracy was usually obtained after 15 iterations for each time step.

2. Examples of results

Comparing the results obtained by different computational methods, we should take it into account that the Frozen Rotor and the Mixing Plane methods are not suitable for the prediction of non-stationary phenomena. Thus, results given by these techniques may be compared only with the time-averaged values obtained by the Sliding Mesh method. According to our investigations, when average values of pressure distribution or velocity values are considered, only the Sliding Mesh and Multiple Reference methods give very similar results, corresponding to the experimental data (presented in part III of this paper). The worst results, remarkably different from the results obtained by the MRF and the SM methods, were obtained by the Mixing Plane method. Moreover, in some cases the Mixing Plane calculations had problems with achieving of the assumed numerical accuracy. These results are not considered and not shown in the examples (Figures 6, 7 and 8).

Figures 6 and 7 present examples of pressure distribution and velocity vectors in the shroud clearance for rotor speed $\omega = 566\text{rad/s}$, for a calculating mesh of type 1 (Figure 4) and for various block interfaces A, B, C (Figure 5) obtained by the MRF and the SM methods, respectively. Figure 8 shows similar results given by the MRF method for block interfaces A and the same velocity but for different types of meshes.

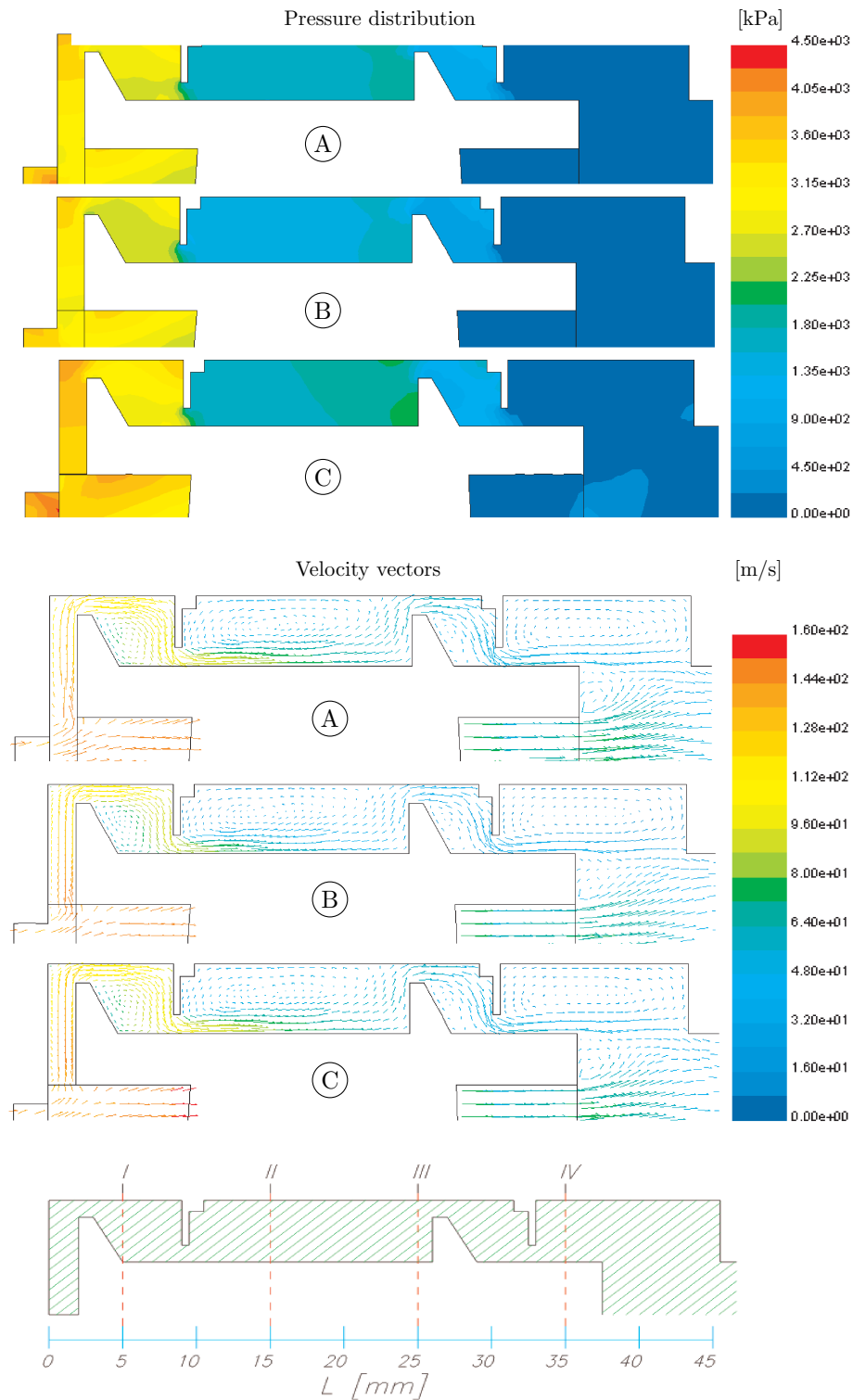


Figure 6. Pressure distribution and velocity vectors in the shroud clearance block interfaces of type A, B and C ($\omega = 566 \text{ rad/s}$, mesh type 1, computational method: MRF)

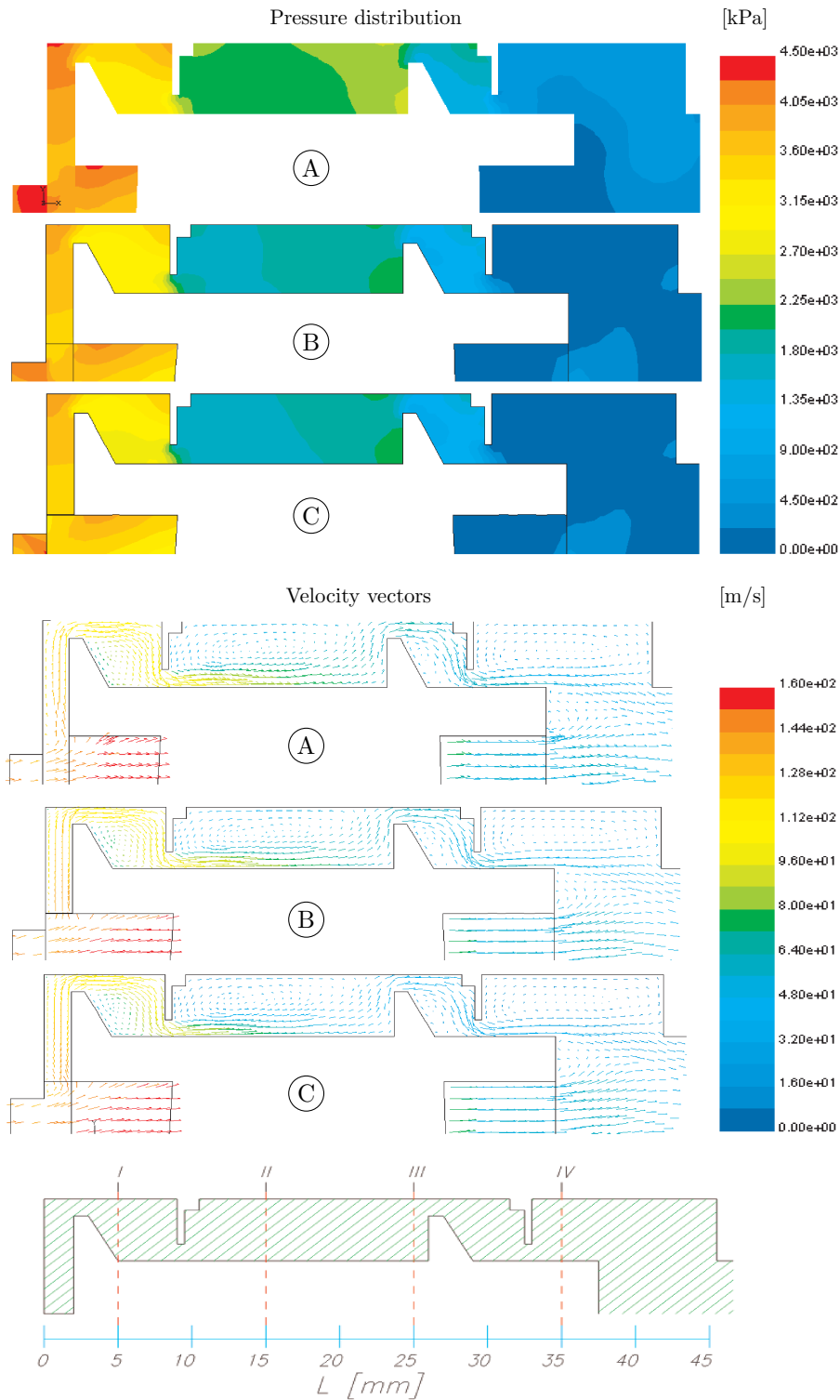


Figure 7. Pressure distribution and velocity vectors in the shroud clearance for block interfaces of type A, B and C ($\omega = 566 \text{ rad/s}$, mesh type 1, computational method: SM)

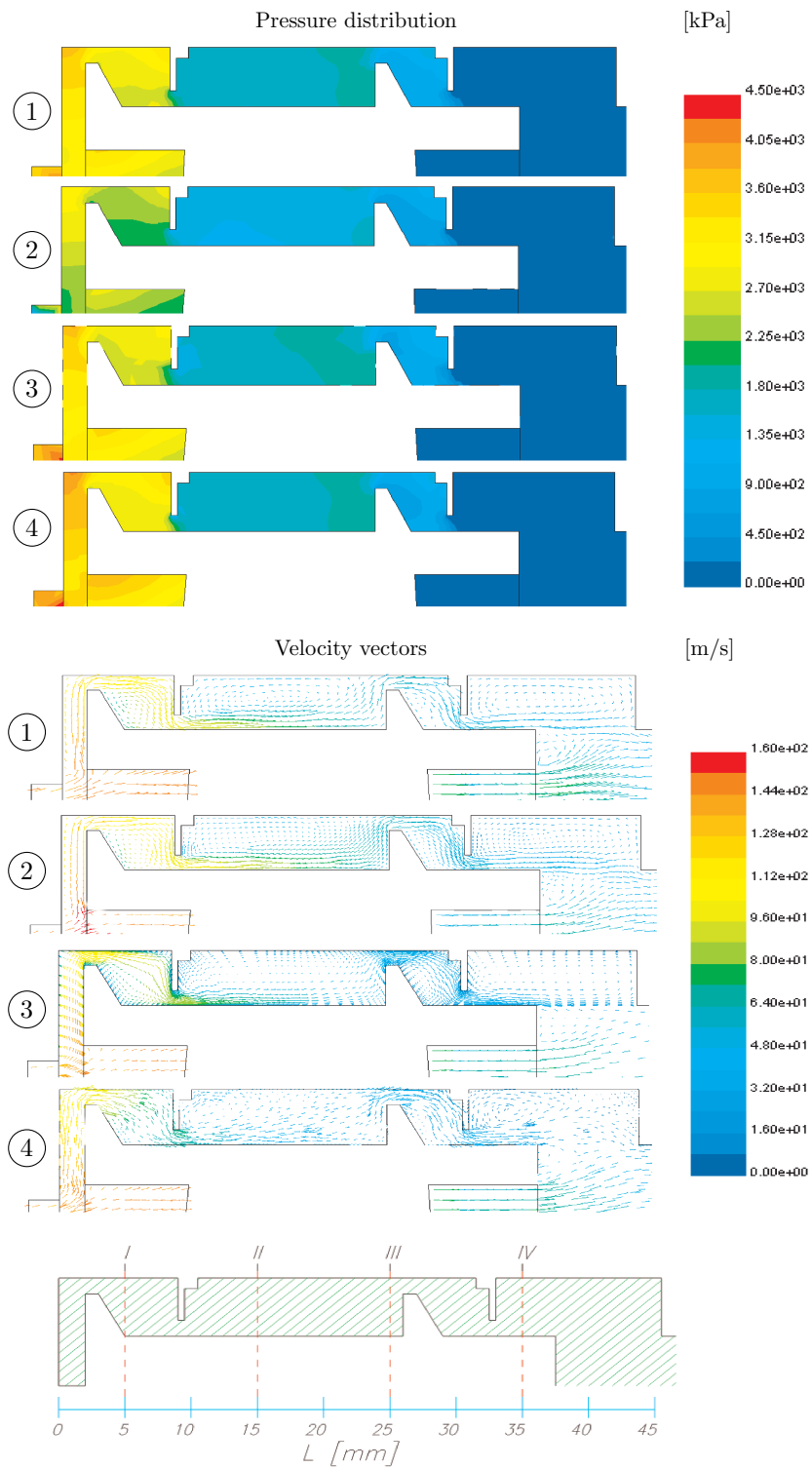


Figure 8. Pressure distribution and velocity vectors in the shroud clearance for meshes of type 1, 2, 3 and 4 ($\omega = 566 \text{ rad/s}$, block interface A, computational method: MRF)



Having analysed the obtained results (examples of which are presented in Figures 6, 7 and 8), we conclude that both the type of the calculating mesh (not to mention the number of cells) and the way of introducing the interfaces between the mesh blocks affect the calculated value of the flow parameters in the shroud seal. This effect is not strong, it primarily concerns quantities and does not remarkably influence the main flow characteristics. But when flows in channels of complicated geometry with very narrow gaps are considered, the type of calculating mesh and the method of block interfaces must be chosen with special care. This may play an important role when problems connected with aerodynamic forces created in turbine seals or problems with generation of energy losses due to leakage and main flow interaction are considered.

3. Conclusions

The Sliding Mesh and the Multiple Reference methods yield very similar results of average values of pressure distribution or the velocity field in the shroud clearance. These results correctly correspond to the experimental data. The pressure pulsations have been determined only by the Sliding Mesh method and these results have also been compared with the experimental ones. For calculations versus experiment see part III of this paper.



